Observations of Mixed-Phase Precipitation within a CaPE Thunderstorm

PAUL L. SMITH, DENNIS J. MUSIL, ANDREW G. DETWILER, AND RAHUL RAMACHANDRAN*

Institute of Atmospheric Sciences, South Dakota School of Mines and Technology, Rapid City, South Dakota

(Manuscript received 29 September 1997, in final form 20 April 1998)

ABSTRACT

Various procedures for inferring hydrometeor characteristics from polarimetric radar data have indicated that regions with echoes exhibiting relatively high linear depolarization ratios along with relatively low differential reflectivity contain wet graupel or hail. Such particles could be found either in a melting zone below the 0°C level in a cloud or in a region of wet growth where the rate of supercooled cloud water accretion overwhelms the rate at which the latent heat associated with complete freezing can be dissipated. In subtropical clouds such as those studied in the Convection and Precipitation/Electrification (CaPE) project in Florida, at the −5°C level or higher, neither condition is obtained. Yet similar polarimetric radar signatures were nevertheless observed at such levels during CaPE.

Examination of in situ observations by the T-28 aircraft in the Florida clouds, along with results from previous laboratory and theoretical studies, suggests that the signature regions were characterized by raindrops formed at lower levels in the clouds in the process of freezing while being carried up in the updraft. This interpretation is supported by some model calculations of the process of raindrops freezing in a supercooled cloud where the particles continue to accrete cloud water. Complete freezing of millimeter-sized drops can take a few minutes after nucleation, and the particles can ascend 1 or 2 km in the updraft during that period.

1. Introduction

With high subcloud water vapor mixing ratios and cloud-base temperatures typically around 20°C, precipitation initially develops in clouds of the Convection and Precipitation/Electrification (CaPE) project region (east-central Florida) via the droplet collision–coalescence mechanism (Pruppacher and Klett 1997). The appearance of ice is an important step in the evolution of these convective clouds. It signals the start of a second branch in the precipitation-formation process, the so-called ice process, that can augment and perhaps supplant liquid-phase coalescence as the dominant mechanism for turning condensate into precipitate in the cell. It also signals the transition from relatively weak electrification to more-active charge separation and potential lightning initiation (e.g., Fitzgerald and Byers 1958; Bringi et al. 1997).

The initial ice could develop in the supercooled parts of the clouds by the nucleation of primary ice particles through one of various mechanisms involving nucleation from vapor or freezing of cloud droplets or raindrops (e.g., Vali 1985; Meyers et al. 1992). The available evidence suggests the latter process, termed coalescence–freezing by Braham (1986), to be more likely in many of these clouds (Beard 1992). This process is difficult to observe in nature, and one result of the CaPE studies in 1991 was to provide further evidence about how it proceeds.

Recent advances in polarization-diversity meteorological radars have led to a capability for remote measurement of some cloud microphysical properties. For instance, Herzegh and Jameson (1992) followed the development of precipitation in warm-based clouds in the southeastern United States using the CP-2 dual-wavelength polarimetric radar. They concluded from depolarization of the 3-cm radar echo from the melting level within a precipitation region, using the linear depolarization ratio (LDR; the ratio of the cross-polarized to the same-sense-polarized return), that there was an LDR ''bright band.'' They further speculated ''. . . that large, tumbling, nonspherical particles such as irregular hail or graupel were present.'' They also said that ''. . . one might speculate that the very high values of LDR found in the precipitation core are suggestive of particles bearing a water coat in a mixed-phase environment.'' Straka and Zrnić (1993) and Höller et al. (1994) have also proposed schemes for inferring hydrometeor characteristics from polarimetric radar data.

* Current affiliation: Atmospheric Science Program, University of Alabama in Huntsville, Huntsville, Alabama.

Corresponding author address: Dr. Paul L. Smith, Institute of Atmospheric Sciences, South Dakota School of Mines and Technology, 501 E. St. Joseph St., Rapid City, SD 57701-3995.
E-mail: psmith@ias.sdsmt.edu

Bringi et al. (1993) and Bringi et al. (1997), among others, have observed enhanced LDR in another context, atop vertical columns of enhanced differential reflectivity (Z_{DR}; the ratio of the reflectivity at horizontal polarization to that at vertical polarization) in Florida's convective clouds during CaPE. They interpreted the "Z_{DR} column" as an updraft containing growing raindrops, following Seliga and Bringi (1976) and Illingworth (1988), and initially interpreted the region of enhanced LDR above as a region of tumbling, nonspherical graupel (initially resulting from frozen raindrops) in wet growth, following Herzegh and Jameson (1992). However, calculations based on the work of Musil (1970) and summarized in Smith et al. (1995) indicate that graupel particles of the observed sizes should be in a dry-growth mode in the observed environments. The latter paper suggested raindrops in the process of freezing as more likely to be responsible for this LDR signature. Bringi et al. (1997) subsequently presented results from particle-scattering calculations showing that the observed LDR signal could be consistent with partially frozen rain, as well as with wet graupel.

We report here on simultaneous in situ photographs and shadowgraphs of precipitation particles and the LDR of the 3-cm radar echo from CP-2 for one CaPE convective storm. We augment these observations with a comparison to some earlier studies of freezing drops and with calculations considering the heat-transfer processes associated with freezing a raindrop that continually accretes supercooled cloud water. Taken together, these considerations make it seem likely that, in this case and probably others, the LDR is due to the presence of these drops in the process of freezing rather than of tumbling graupel in wet growth.

2. Some previous studies of raindrop freezing

Blanchard (1957) pioneered the study of the freezing of freely falling large drops (~8-mm diameter) using a small outdoor vertical wind tunnel. He was able to observe the drops as they froze, a process that could take several minutes, as well as to remove frozen or partially frozen drops from the airstream and photograph them. He observed two different patterns of drop freezing. When the wet-bulb temperature was above −4° to −5°C, "... a shell of ice, first forming on the bottom of the drop, will envelop the drop and then freeze inward." The ice portions of the partially frozen drops, of which he gives example photographs, were decidedly irregular. When the wet-bulb temperature was below −4° to −5°C, "... the freezing appears to occur nearly simultaneously over the entire surface of the drop causing the drop to turn an opaque white." Blanchard further noted that drops would often remain supercooled for 10 min or longer at −5°C, while at −8°C the supercooled state did not generally extend beyond a minute. This difference probably reflects the likelihood of capturing an active ice nucleus at the respective temperatures.

Mason and Maybank (1960), Dye and Hobbs (1968), and Johnson and Hallett (1968) discussed the process of drop freezing, as did Knight and Knight (1974); in each instance the focus was on the question of drop splintering or shattering, though Johnson and Hallett provided some information on drop-freezing times. Sassen (1977) reported observations of drops during the freezing process, made in the course of a laboratory study of light scattering by hydrometeors. Some of these investigators also noted that the progressive drop-freezing process began with the formation of an ice shell.

Relevant theory and observations summarized in Pruppacher and Klett (1997) suggest drop-freezing times around 1 min. Sassen shows an example of a static 2.1-mm drop freezing in just over 1 min at −5°C. However, none of those earlier studies took into account the ongoing accretion of supercooled cloud water that would be occurring in updrafts of real clouds.

3. T-28 observations from Florida clouds

More recently, drops in the process of freezing inside clouds were photographed in situ using the Cannon particle camera (Cannon 1974) on the South Dakota School of Mines and Technology T-28 storm-penetrating aircraft. These observations occurred during two field seasons in the Kennedy Space Center area of Florida (the Thunderstorm Research International Project 1978, and CaPE 1991).

Figure 1 presents a multipanel view of a multicellular Florida convective storm that occurred on 29 July 1991. Ramachandran et al. (1996) have studied the electrification of this storm. On this day, the cloud-base height was around 1.2 km above mean sea level (MSL) and the 0°C level was near 4.6 km MSL. Figure 1a shows a constant-altitude plan position indicator (CAPPI) view just after 2200 UTC of CP-2 10-cm radar reflectivity factor Z at 6 km MSL with the path of the T-28 aircraft, penetrating near this level, superimposed. The aircraft penetrated from southwest to northeast, passing through three identifiable convective cells, labeled A, B, and C. At this time, A is the oldest cell and C the newest.

Figure 1b shows a vertical cross section of 10-cm Z_{DR} along the aircraft flight track. The measured vertical wind and cloud liquid water concentration (LWC) along the aircraft track are plotted above to the same horizontal distance scale. Separate updraft regions, associated with the three convective cells, are labeled A, B, and C. The region of high Z_{DR} extending above the flight level in cell C constitutes a Z_{DR} column. This cell also contained LWC approaching 4 g m^{-3} at the T-28 flight level; that was the greatest LWC observed by the T-28 in any of its 259 CaPE cloud penetrations.

Figure 1c shows a corresponding vertical cross section of 3-cm LDR along the aircraft track. Plotted above are the measured ambient temperature and the count rate (an indicator of particle concentration) from a Particle Measuring Systems (PMS) OAP 2D-P precipitation–

particle probe carried by the T-28. The penetration was through the supercooled part of the cloud, with temperatures ranging from −5° to −8°C. Cell B contained precipitation particles within and at the edges of the updraft, but most of the precipitation in cell C was at the updraft edges. No region of strong depolarization is associated with cell A, but a region of enhanced depolarization is centered just below the aircraft level within cell B. In cell C, another such region is centered just above the aircraft level and atop the Z_{DR} column shown in Fig. 1b.

Figure 2 shows echo time–height histories of Z, Z_{DR}, and LDR for cell C, compiled from CP-2 sector range–height indicator (RHI) scans (Ramachandran et al. 1996). The 2-dB Z_{DR} contour is highlighted and the upper region with LDR >-21 dB is hatched. The 2-dB Z_{DR} contour rises to 6 km by 150 s in the plot (i.e., about 2202 UTC), as rain develops in the updraft. (The T-28 was in cell C from about 225 to 260 s on this plot.) Enhanced LDR appears at the 6.5-km level (−10°C in the environment) at 200 s, possibly indicating the initial freezing of rain. This region of enhanced LDR first expands and rises, then descends. A second maximum appears at the melting level after 400 s. These regions would be identified as containing either wet graupel, in wet growth (above) or melting (below), according to the schemes of Herzegh and Jameson (1992) or Straka and Zrnić (1993), or wet or spongy hail, according to the interpretation of Höller et al. (1994).

Figure 3 shows selected (every eighth second) particle images on this penetration from the 2D-P probe carried by the T-28. Rough and quasi-circular images up to about 2 mm in diameter, suggestive of rimed graupel, were found in cell A. A mixture of these same types of images along with a few larger elongated images, characteristic of liquid drops, was found in cell B. The cell C portion of the penetration shows the same small particles and many streaked images due to cloud water collecting on the probe tips and then shedding, along with one definite and one probable large raindrop image.

Figure 4 shows sample photographs of in-focus particles from the Cannon particle camera, in which two strobe lamps illuminate particles in the field of view obliquely from behind (Cannon 1974). The dot-pair signature of the large particle in Fig. 4a is characteristic of a liquid drop; the drop acts as a lens to produce point images of the two lamps with a separation proportional to drop size. The milky white image in Fig. 4c represents an ice particle. The intermediate particle image in Fig. 4b exhibits only one of the pair of dots, with an opalescent character over the opposite side of the particle; we interpret this to be a drop in the process of freezing (see section 5). Dozens of images also intermediate between Figs. 4a and 4c from this penetration, and large numbers from other Florida cases, give further indications of precipitation particles in transition from the liquid to the ice phase. These photos show that partially frozen raindrops are present in mixed-phase regions of the CaPE clouds.

4. Model calculations

The following available evidence suggests the occurrence of partially frozen raindrops in CaPE clouds: 1) the T-28 hydrometeor observations, which are in effect snapshot views, and 2) drop-freezing calculations and experiments indicating that several minutes can be required to freeze large supercooled drops. The freezing is not instantaneous because of the need to dispose of the latent heat before a drop can freeze completely, a requirement exacerbated by the ongoing accretion of supercooled cloud water. To assess the drop-freezing process more fully, calculations were made using an adaptation of a model developed by Dennis and Musil (1973).

a. Description of the model

The original model was designed to study questions related to the growth of hail, but it had several features that allow its application to Florida clouds. These include a collision–coalescence process and the freezing of liquid hydrometeors. The version of the model described here assumes that spherical particles are growing in an environment specified mainly by profiles of cloud liquid water concentration, updraft speed, and temperature. It is a continuous-growth model that follows single particles as each moves vertically through the model cloud, growing by coalescence in ''warm'' regions and essentially by accretion at ''cold'' temperatures. The purpose of the analysis is to explore the characteristics of the drop-freezing process and test whether such a simple model can produce conditions compatible with some of the features observed in the Florida clouds, especially in the region above the 0°C level.

The program calculates quantities pertinent to a growing and freezing raindrop, such as size and fraction of water, as well as time and vertical distance traveled in the model cloud. The mass and heat budgets for the freezing particle are described through a series of equations treating the accretion of supercooled cloud droplets and the collection of cloud ice crystals. Heat exchanges are controlled through the processes of conduction, evaporation, accretion, and collection of cloud ice. The particle is assumed to have a uniform temperature of 0°C during the freezing process and its density is assumed to vary in a linear fashion between 1 g cm^{-3}, when liquid, and 0.9 g cm^{-3}, when frozen.

Heat is conducted away from the freezing particle when it is warmer than the cloud environment, which will usually be the case in the model because the freezing particle at 0°C will usually be rising above the 0°C isotherm and accreting mass in the updraft containing supercooled cloud water. The accretion term generally has the largest magnitude in heat or mass exchanges

(a)

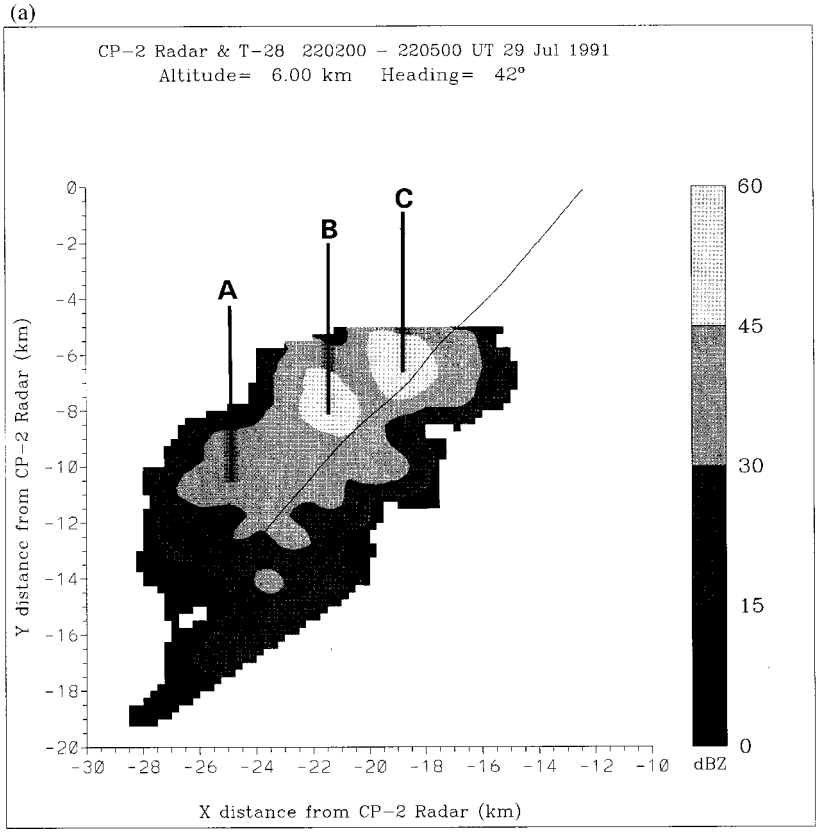

(b)

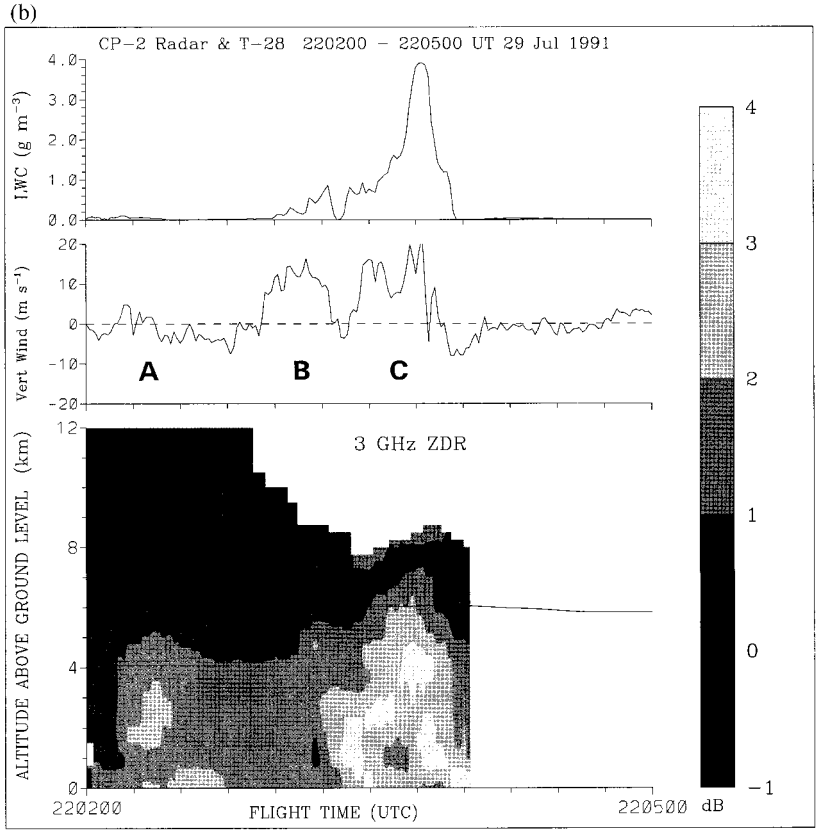

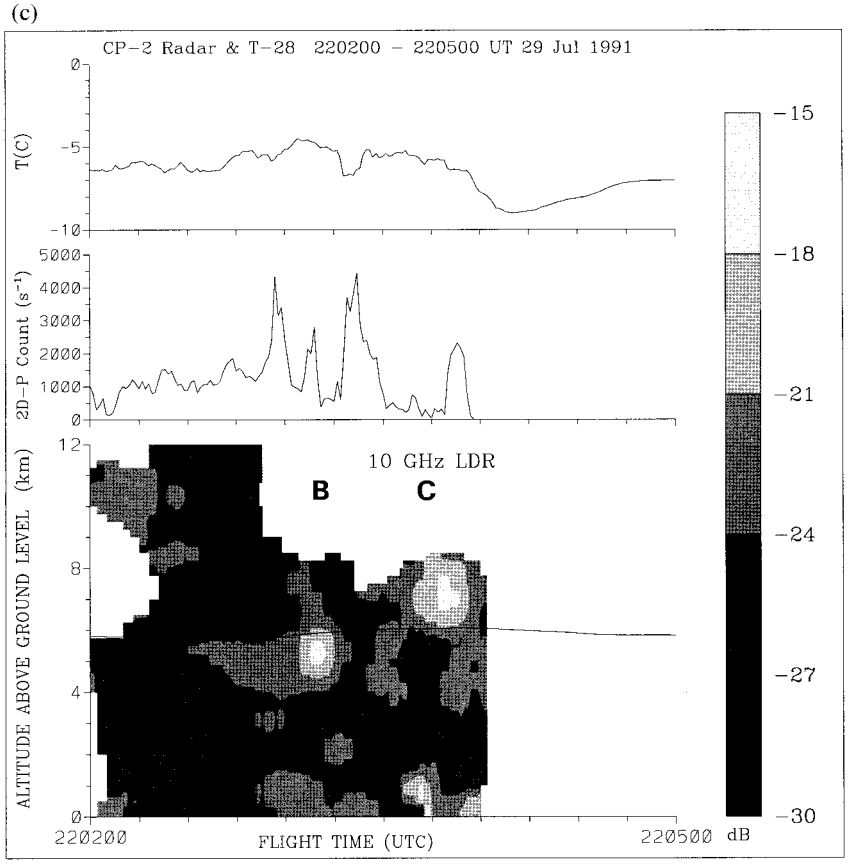

FIG. 1. Radar and aircraft view of 29 July 1991 storm with cells A, B, and C labeled. (a) CP-2 CAPPI section at 6.0 km MSL, with T-28 flight track superimposed; shading indicates reflectivity factors (dBZ). (b) Vertical cross section of CP-2 differential reflectivity (shading indicates values in dB) along T-28 track; 1 min along the timescale corresponds to about 5.5 km of flight. Plots above show vertical winds and cloud LWC measured by the Johnson–Williams cloud water meter on the aircraft. (c) Vertical cross section of CP-2 LDR (shading indicates values in dB) along T-28 track; timescale as in (b) with plots above indicating aircraft-measured temperature and precipitation-particle count rate from the PMS 2D-P probe. The 2D-P samples $\sim$0.16 m^3 s^{-1} and detects particles larger than 0.2-mm diameter.

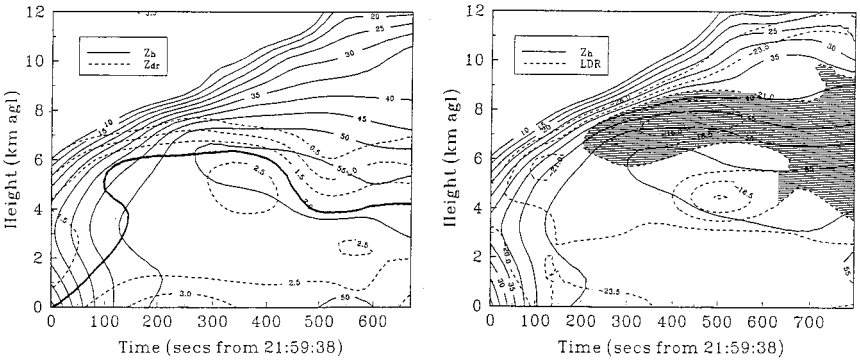

FIG. 2. Radar time–height cross section of cell C in 29 July 1991 storm; solid contours indicate reflectivity factors in dBZ. Left: Dashed contours indicate Z_{DR} (dB) with 2-dB contour highlighted. Right: Dashed contours indicate LDR (dB) with significant region having values >-21 dB shaded.

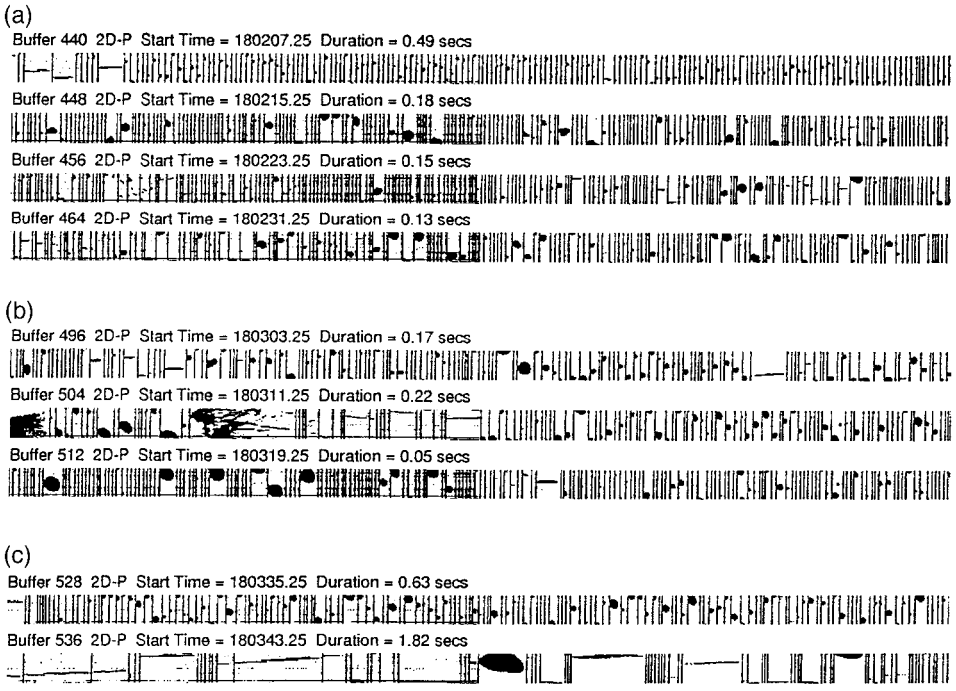

FIG. 3. Sample PMS 2D-P probe images of precipitation particles from cells A, B, and C of the 29 July 1991 storm. Vertical bars between images represent vertical scale of 6.4 mm.

and involves both the latent and sensible heat in the accreted water. The term is always positive under the conditions involved in this study, so heat is added to the particle. The collection term involves the sensible heat of the collected ice crystals, which should be near the temperatures found in the cloud. Since the freezing particle is assumed to have a temperature of 0°C, the ice crystals will always serve to cool it and aid the freezing process. Mass exchanges due to ice crystal collection should be small because few ice crystals would be found in the region of interest. The contribution of the evaporation term to the heat budget can be either positive or negative but is probably negligible for the large-sized particles considered in this study.

b. Special model features

To estimate in-cloud conditions, the model calculated the pertinent pseudoadiabat passing near the observed cloud base as given by height, temperature, and pressure on 29 July 1991. The cloud-base conditions, mentioned previously, were estimated from several radiosondes released at Cape Canaveral Air Force Station on that day; all had similar properties. The expression given in Hess (1959) was used with small height steps to approximate the pseudoadiabat. The temperatures along it were within about 0.5°C of values found on the Skew T diagram. Values of adiabatic cloud liquid water concentration were found using the conditions along the pseudoadiabat. Accuracies to within a fraction of a degree in temperature lead to LWC values that are within about 1%–2% of adiabatic values. The LWC can only be measured to within about 20%, so the accuracy for this study is more than adequate.

The simulated pseudoadiabat provided near-adiabatic temperatures that were higher than the T-28-observed temperatures (which could be low due to the sensor

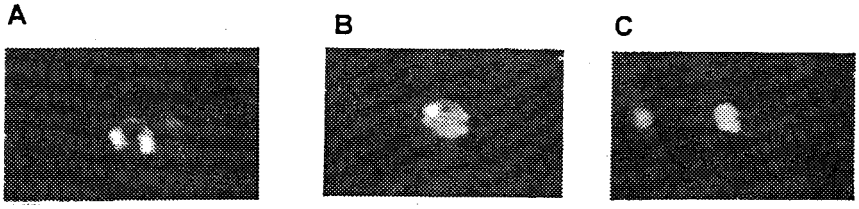

FIG. 4. Examples of Cannon camera photographs from the 29 July 1991 storm; particles shown approximately 1.5 times actual size. (a) A large raindrop; (b) a particle in transition from liquid to ice; and (c) an ice particle. The first two photos were taken in weak updraft on the southwest side of cell B (comparable photos were not obtained in cell C because the particle concentrations were too low at this time); the photo in (c) was taken in weak downdraft in cell A.

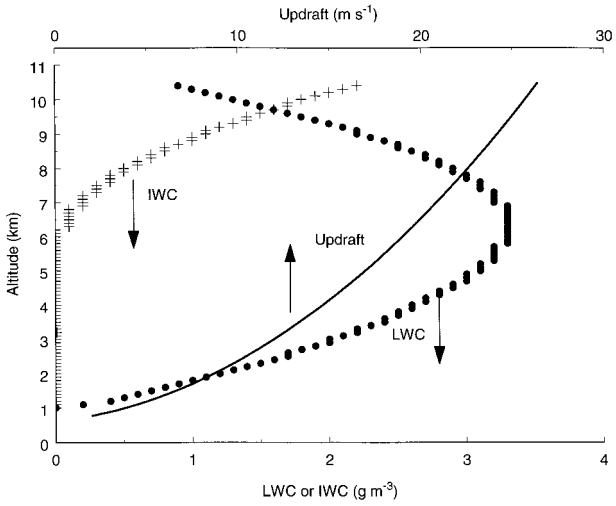

FIG. 5. Plot of LWC and ice mass IWC concentrations (g m^{-3}) and updraft speed (solid line) as a function of height in the model cloud simulating observed LWCs.

wetting that is suggested by the temperature trace in Fig. 1c as the aircraft exits the cloud). It also gave adiabatic cloud LWC values substantially higher than those observed (see Fig. 1b). The observed LWC values probably somewhat underestimate true values due to incomplete response of the Johnson–Williams cloud-water meter to the broad droplet spectrum typical of Florida clouds. The cloud LWC values in the model were reduced by 50% to provide better agreement with actual observations by the T-28. The temperatures were reduced by 1.5°C from the adiabatic values to approximate the lower temperatures measured by the T-28. These adjustments reflect in the model the effects of entrainment and cloud-water depletion by precipitation in the actual storm. Furthermore, the cloud liquid was frozen by a temperature-dependent percentage according to a square-law expression over the temperature range from 0°C to −40°C. This allows for a slow-starting, nonlinear freeze-up of cloud water as temperatures decrease below 0°C, where the cloud water would be about 50% frozen by −30°C. This droplet-freezing process is similar to ones used in more complex cloud models (e.g., Lin et al. 1983) and provides a reasonable approximation to the amounts of cloud ice for our purposes.

The effects of heat and mass exchanges due to the collection of ice crystals were incorporated into the model, even though it was recognized that the cloud ice concentrations are low and they would be minor in the region of main interest (between 0° and −10°C). Figure 5 shows the values for cloud LWC and cloud ice concentration in the resulting model along with the model updraft profile. Cloud ice begins to appear in measurable amount at about the 6.5 km (−7°C) level and is about equal to the amount of cloud liquid near 10 km. The collection efficiency for the cloud ice is taken to be 1, as the wet nature of the freezing drops should allow them to collect any ice crystals that are encountered.

The appendix briefly discusses two minor factors, collection of raindrops and shedding by partially frozen particles, which are not important under the conditions considered here.

c. Results

An examination of values from the heat balance equations indicates that for smaller particles introduced in the model cloud, the net heat gained by accretion is about the same order of magnitude as heat losses due to conduction and evaporation. Losses due to collection of ice particles are much smaller. Thus the drop freezing will tend to proceed more slowly in the cloud than in the previous studies summarized in section 2. With the introduction of larger particles, or when growth has achieved larger sizes, one begins to see the larger cross-sectional area producing a stronger accretion effect. Thus, the larger the particle, the more difficult it is for it to freeze in any region with substantial cloud liquid water concentrations; the larger particles also grow much faster. The hydrometeor contributions to Z_{DR} and LDR tend to be reflectivity weighted, hence dominated by the larger particles, which take longer to freeze. The raindrop freeze-up (and hence, the structure of the Z_{DR} and LDR profiles) reflects some balance between the profiles of temperature, vertical wind, and liquid water concentration in the cloud and the sizes of the freezing particles.

1) FREEZING OF DROPS

Using the cloud liquid water and ice mass concentrations shown in Fig. 5, which approximate the observed cloud conditions, drops ranging in diameter from 0.5 to 5 mm were introduced into the model environment near the −5°C level (~6 km). Freezing was assumed to begin upon introduction, and each drop was allowed to grow for an arbitrarily specified 400 s or until it became completely frozen, whichever came first. Figure 6 shows an example of the fate of the 3.2-mm drop, which was the largest one introduced that became completely frozen in 400 s. The particle achieved an altitude above 8 km with a final diameter near 15 mm before it was completely frozen by the end of the time period. All drops with initial sizes less than 3.2 mm were completely frozen at various times less than 400 s, while the larger ones were only partially frozen before the arbitrary cutoff.

A summary of the results for these runs is given in Fig. 7 (solid lines), which shows the time required to freeze, the height achieved at freeze-up, and the final diameter as a function of initial drop size. As mentioned above, all drops with initial sizes less than or equal to 3.2 mm froze during times ranging between about 10 and 400 s. The altitudes achieved by the drops at freeze-

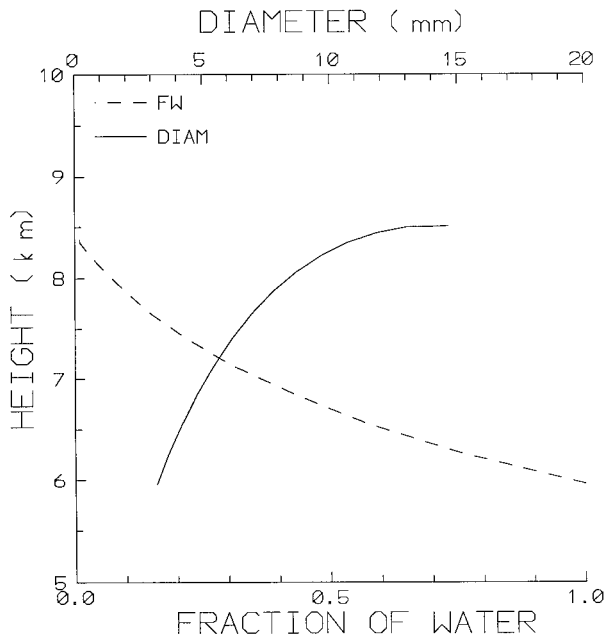

FIG. 6. Plot of liquid-water fraction and particle size vs height in the model cloud for a 3.2-mm drop nucleated at the −5°C level and completely frozen after 400 s.

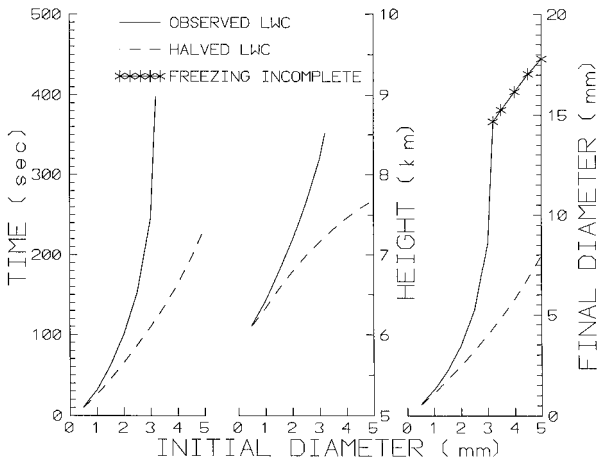

FIG. 7. Summary of model results for freezing drops of various initial sizes, nucleated at the −5°C level in the model cloud with the ''observed'' cloud LWC profile (solid lines) and with half that amount of cloud water (dashed lines). Left: time needed to complete the freezing process. Center: height attained at the time of complete freezing. Right: final size of growing particle upon complete freezing.

up are a direct function of their initial sizes; drops larger than about 2 mm remain incompletely frozen above the height of the center of the ''enhanced-LDR region'' in cell C (Fig. 1c or Fig. 2). The larger particles have grown enough during their trajectories that they are about ready to descend in the updraft, which in the model is steady state. The final sizes at this time have reached more than 15 mm.

No attempt was made to follow the particles during their descent, or for that matter, beyond their freeze-up point. In the case of the former, the one-dimensional nature of the model environment would involve much additional growth as the particles descend, producing unreasonably large particles. With its steady-state structure, this version of the model cannot realistically treat questions related to such things as cloud water depletion or the nonsteady-state nature of the updrafts in real clouds.

2) EFFECTS OF CLOUD LIQUID WATER

A similar series of model runs were made with the liquid and ice concentrations of Fig. 5 cut in half to investigate further the effects of liquid water concentrations. During these runs, with reduced cloud LWC, the drops froze significantly faster, and all drops up to about 5 mm initial size became completely frozen during the 400-s time period (Fig. 7). Those results reflect the lower amounts of latent heat added to the drops as a result of smaller accretion in the second set of runs. The heights achieved by the larger drops begin to level off near 7.5 km during this second set of runs.

Figure 8 shows the height where freezing was completed as a function of initial drop size, with the cloud liquid set to zero in the model. The curves are for two starting points, around the 0°C level and around −5°C in the modified adiabatic profile. Nucleation to initiate the freezing process at 0°C in the updraft is unlikely, so the −5°C curve is probably more representative of the actual situation. All drops were frozen by the time the particles reached about 7 km; drops beginning to freeze lower in the cloud, at higher temperatures, would complete the freezing process at an even lower height. The largest drops ascended by nearly a kilometer, or more, during the freezing process.

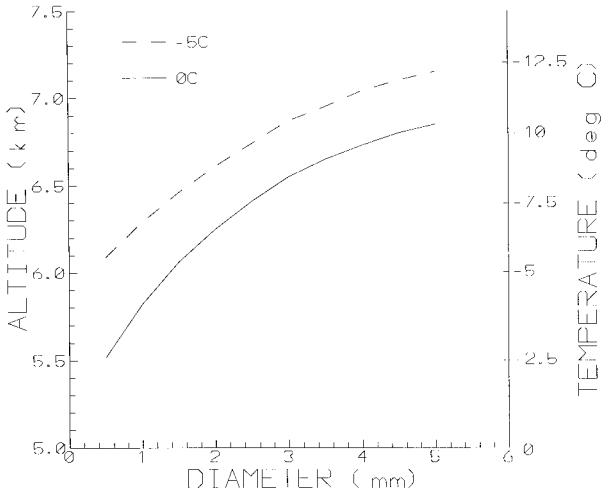

FIG. 8. Plot of heights (MSL) and temperature levels where drops of various initial sizes, nucleated in the model cloud at the 0°C or −5°C level and ascending in an updraft containing no cloud water, would become completely frozen.

The times required for drops to freeze (not shown for the zero-LWC case) are again a direct function of the initial drop size, but the times are substantially shorter when the drops begin to freeze at a lower temperature. Even over the small difference of temperatures used here for initiating freezing, the smallest drops freeze in about one-third of the time starting at the lower temperature, while the largest freeze in about one-half of the time. Overall, the times to complete freezing range from about 10 s to over 4 min; these values are very similar to the observations made by Blanchard (1957) or Sassen (1977). A test with a static (no ventilation due to its fallspeed) 2.1-mm drop gave a 70-s freezing time, which compares well with Sassen's laboratory observation.

Tests also were made for the opposite extreme, using unmodified adiabatic cloud LWCs and temperatures. The model grew particles much larger than anything observed in the actual cloud, and few of the drops could be frozen completely, even at extremely low temperatures (i.e., less than -30°C). It became obvious that the freezing process is difficult to complete with adiabatic conditions, and that a mechanism like that indicated in section 4b for representing the lower observed amounts of cloud water is necessary. Even with that, some of the larger drops still had difficulty freezing in the model. This runs somewhat counter to the observations, which indicate that most of the precipitation-sized particles in Florida clouds have frozen by the time they reach about the -10°C level. This provides a further indication that adiabatic cores are rare in mature Florida thunderstorms.

3) EFFECTS OF CLOUD ICE

As expected, there was little effect from the inclusion of cloud ice for mass and heat exchange purposes in the model. There is little cloud ice in the temperature region from 0° to -10°C, which is where the model particles spent most of the time. The largest cloud ice concentration observed in any of the runs described here was about 0.2 g m^{-3}, and it was usually much lower. Nevertheless, any amounts of cloud ice present would aid in the drop-freezing process because the cloud ice would have a lower temperature than the freezing drops.

5. Discussion

The T-28 observations in the mixed-phase regions of Florida clouds have shown the presence of drops in the process of freezing. In Fig. 3, the more symmetrical images, if rough, are interpreted as ice particles. They fall more slowly than liquid particles of the same size and do not appear elongated in 2D-P shadowgraphs. On the other hand, large raindrops, being generally nonspherical and falling at a significant rate compared to the true airspeed of the aircraft ($\sim$90 m s^{-1}), appear elongated in these images (e.g., Chandrasekar et al. 1988). The in situ photographs in Fig. 4 clearly show a variety of particle states. Included are transparent, liquid drops; opaque particles that are frozen completely, at least at the surface; and what we interpret to be drops in the process of freezing, with both a distinguishable frozen portion and a liquid portion. Such partially frozen drops would probably be more nearly circular than completely liquid drops of similar size and thus could appear to be frozen in 2D-P shadowgraphs such as those in Fig. 3. Laboratory observations and model calculations of the time required to freeze large raindrops support the likelihood of finding partially frozen drops in these clouds.

Liquid surrounding ice would produce much stronger radar depolarization than particles of similar size and shape comprising liquid encased within an ice shell. A partially frozen, incompletely encased drop would have an irregularly shaped ice portion around which the liquid portion might oscillate. Such oscillation could be due to tumbling of the particle, shedding of eddies in its wake, turbulence in the air through which the particle is falling, or nonequilibrium motions of the ensemble of liquid and ice. Sassen (1977) also observed the extrusion of liquid from within the ice shell during the drop-freezing process. This partially frozen state might last for a minute or more, according to the observations of Blanchard and Sassen and the model computations discussed above. Moreover, the drops in an ensemble comprising a range of sizes would begin to freeze at different times. Thus we believe that this transition state, with ice portions of the particles growing slowly as the liquid portions diminish, may be responsible for the upper LDR signal observed in the CaPE storms. The scattering-model calculations summarized in Bringi et al. (1997) are consistent with this view. This LDR signature may occur in conditions where the cloud water that could be collected by the falling particles would not be sufficient to maintain a completely frozen surface in a state of wet growth. The lower LDR region in the right panel of Fig. 2, on the other hand, probably results from the melting process as suggested by Herzegh and Jameson (1992).

6. Summary

Laboratory and in situ observations as well as analytical and numerical computations suggest that depolarization of linearly polarized radar signals backscattered from regions atop updraft cores in Florida thunderstorm cells results when raindrops freeze relatively slowly. During the freezing process, some of the unfrozen liquid may slosh around the initially frozen ice portion, leading to a liquid-coating-ice formation somewhat analogous to the case of melting hail and graupel. However, at the observed temperatures (<-5°C) melting of the particles is not a factor. The cloud water concentration in these cases is unlikely to be sufficient to maintain an ice-particle surface in a state of wet growth. Thus the interpretation of radar LDR signatures

may have to allow for the possibility of raindrops in the process of freezing.

Acknowledgments. This material is based upon work supported by the National Science Foundation under Grants ATM-9022846 and ATM-9509810 and Cooperative Agreements ATM-9104474 and ATM-9401117. We appreciate the assistance of V. N. Bringi in the processing and interpretation of the CP-2 radar observations. The 2D-P precipitation particle images were obtained with an instrument loaned by the Atmospheric Environment Service of Canada for use on the T-28 aircraft during CaPE.

APPENDIX

Minor Factors in Drop-Freezing Model

a. Collection of raindrops

The effects of the possible collection of raindrops were not considered in this study. If there are collisions between the freezing raindrop and other raindrops, the freezing process would be slowed and the effect of drop breakups would also have to be considered. However, it is unlikely that there would be many drop collisions because the growing particles in this model would be developing in updrafts with low drop concentrations. The range of drop sizes is likely to be narrower than that in a fully developed drop spectrum, reducing the chances for collisions.

b. Shedding

The model used by Dennis and Musil (1973) includes a shedding routine. However, that routine is not needed here because the particles considered are small. This study begins with small liquid drops and follows the growth and freeze-up of the relatively small particles as they rise in the updraft. Due to dynamic instability considerations, the model has a 5-mm critical diameter for the breakup of raindrops; only those larger than 5 mm would need to be considered for the possibility of shedding excess accreted cloud liquid. However, breakup considerations are not germane to the freezing process and are not pursued here.

Following the work of Dennis and Musil (1973), it was found that even those particles larger than 5 mm are not likely to grow large enough that shedding can begin. For example, a 5-mm raindrop introduced at the -5°C level in the model cloud and allowed to grow for about 6 min reaches a diameter of about 15 mm with a fraction of water about 0.4. Even this relatively large particle will not satisfy the condition for shedding established by Dennis and Musil at any time during its growth. It follows that introducing smaller raindrops would produce similar results. Thus, for the particles used in this study, one can assume that a lattice-type structure described by List (1960) will develop as the drop freezes and all the accreted mass will stay with the growth particle.

REFERENCES

Beard, K. V., 1992: Ice initiation in warm-based convective clouds: An assessment of microphysical mechanisms. *Atmos. Res.,* **28,** 125–152.

Blanchard, D. C., 1957: Supercooling, freezing and melting of giant water-drops in air. *Artificial Stimulation of Rain. Proc. First Conf. on the Physics of Cloud and Precipitation Particles,* H. Weickmann and W. Smith, Eds., Pergamon Press, 233–249.

Braham, R. R., 1986: The cloud physics of weather modification. Part I: Scientific basis. *WMO Bull.,* **35,** 215–221.

Bringi, V. N., A. Detwiler, V. Chandrasekar, P. L. Smith, L. Liu, I. J. Caylor, and D. J. Musil, 1993: Multiparameter radar and aircraft study of the transition from early to mature storm during CaPE: The case of 9 August 1991. Preprints, *26th Int. Conf. on Radar Meteorology,* Norman, OK, Amer. Meteor. Soc., 318–320.

——, K. Knupp, A. Detwiler, L. Liu, I. J. Caylor, and R. A. Black, 1997: Evolution of a Florida thunderstorm during the Convection and Precipitation/Electrification experiment: The case of 9 August 1991. *Mon. Wea. Rev.,* **125,** 2131–2160.

Cannon, T. W., 1974: A camera for photography of atmospheric particles from aircraft. *Rev. Sci. Instrum.,* **45,** 1448–1455.

Chandrasekar, V., W. A. Cooper, and V. N. Bringi, 1988: Axis ratios and oscillations of raindrops. *J. Atmos. Sci.,* **45,** 1323–1333.

Dennis, A. S., and D. J. Musil, 1973: Calculations of hailstone growth and trajectories in a simple cloud model. *J. Atmos. Sci.,* **30,** 278–288.

Dye, J. E., and P. V. Hobbs, 1968: The influence of environmental parameters on the freezing and fragmentation of suspended water drops. *J. Atmos. Sci.,* **25,** 82–96.

Fitzgerald, D. R., and H. R. Byers, 1958: Aircraft observations of convective cloud electrification. *Recent Advances in Atmospheric Electricity,* L. G. Smith, Ed., Pergamon Press, 245–268.

Herzegh, P. H., and A. R. Jameson, 1992: Observing precipitation through dual-polarization radar measurements. *Bull. Amer. Meteor. Soc.,* **73,** 1365–1374.

Hess, S. L., 1959: *Introduction to Theoretical Meteorology.* H. Holt and Co., 362 pp.

Höller, H., V. N. Bringi, J. Hubbert, M. Hagen, and P. F. Meischner, 1994: Life cycle and precipitation formation in a hybrid-type hailstorm revealed by polarimetric and Doppler radar measurements. *J. Atmos. Sci.,* **51,** 2500–2522.

Illingworth, A. J., 1988: The formation of rain in convective clouds. *Nature,* **336,** 754–756.

Johnson, D. A., and J. Hallett, 1968: Freezing and shattering of supercooled water drops. *Quart. J. Roy. Meteor. Soc.,* **94,** 468–482.

Knight, C. A., and N. C. Knight, 1974: Drop freezing in clouds. *J. Atmos. Sci.,* **31,** 1174–1176.

Lin, Y.-L., R. D. Farley, and H. D. Orville, 1983: Bulk parameterization of the snow field in a cloud model. *J. Climate Appl. Meteor.,* **22,** 1065–1092.

List, R., 1960: Growth and structure of graupel and hailstones. *Physics of Precipitation, Geophys. Monogr.,* No. 5, Amer. Geophys. Union, 317–324.

Mason, B. J., and J. Maybank, 1960: The fragmentation and electrification of freezing water drops. *Quart. J. Roy. Meteor. Soc.,* **86,** 176–185.

Meyers, M. P., P. J. DeMott, and W. R. Cotton, 1992: New primary ice nucleation parameterizations in an explicit cloud model. *J. Appl. Meteor.,* **31,** 708–721.

Musil, D. J., 1970: Computer modeling of hailstone growth in feeder clouds. *J. Atmos. Sci.,* **27,** 474–482.

Pruppacher, H. R., and J. D. Klett, 1997: *Microphysics of Clouds and Precipitation.* Kluwer Academic, 954 pp.

Ramachandran, R., A. Detwiler, J. Helsdon Jr., P. L. Smith, and V.

N. Bringi, 1996: Precipitation development and electrification in Florida thunderstorm cells during Convection and Precipitation/Electrification Project. *J. Geophys. Res.,* **101,** 1599–1619.

Sassen, K., 1977: Optical backscattering from near-spherical water, ice and mixed phase drops. *Appl. Opt.,* **16,** 1332–1341.

Seliga, T. A., and V. N. Bringi, 1976: Potential use of radar differential reflectivity measurements at orthogonal polarizations for measuring precipitation. *J. Appl. Meteor.,* **15,** 19–76.

Smith, P. L., A. G. Detwiler, D. J. Musil, and R. Ramachandran, 1995: Observations of mixed-phase precipitation within a CaPE thunderstorm. Preprints, *Conf. on Cloud Physics,* Dallas, TX, Amer. Meteor. Soc., 8–13.

Straka, J. M., and D. S. Zrnic, 1993: An algorithm to deduce hydrometeor types and contents from multi-parameter radar data. Preprints, *26th Int. Conf. on Radar Meteorology,* Norman, OK, Amer. Meteor. Soc., 513–515.

Vali, G., 1985: Atmospheric ice nucleation—A review. *J. Rech. Atmos.,* **19,** 105–115.